A NOVEL USE OF REMOTE SENSING TO IDENTIFY FAVORABLE *POPULUS DELTOIDES* RECRUITMENT AREAS AT THE REACH-SCALE IN A HUMID SUBTROPICAL SYSTEM

by

Kevin Louis Casula

A professional paper submitted in partial fulfillment
of the requirements for the degree

of

Master of Science

in

Land Resources and Environmental Sciences

MONTANA STATE UNIVERSITY
Bozeman, Montana

May 2022

ACKNOWLEDGEMENTS

Foremost, I could not have completed this degree without the support of my beautiful wife, Jennifer Casula. I cannot thank you enough for your help, patience and support in my pursuit of this degree! You are awesome!

I'd like to express my most sincere gratitude and appreciation toward Dr. Sam Carlson. His willingness to take on the role of being my advisor, the amount of time he was able to devote to my endless questions, and having his buddy Oscar to help us out from time to time. Thank you, I look forward to working with you to make this project even better!

To the LRES staff, thank you for being the kind, respectful, and insightful people that you are. You are truly the face of this program and are the reason why this program is so successful. You definitely made 'going to school' fun! Thank you! To all my classmates, your discussions and perspectives helped me tremendously! Thank you and good luck!

I'd like to acknowledge the management and staff of Backbone Valley Nursery (Marble Falls, TX) for their understanding and patience as I worked toward completing this degree as well as the numerous questions and insights offered along the way. Thank you very much!

Thank you to my father, David, and his wife, Margaret for letting me hijack your kitchen table so I could work on this project! Thank you for your support! Same goes for my in-laws, Jimmy and Joy, thank you for your patience and support as I pursued this degree!

A special thanks to two of my fur-babies, Spike and Leila, who served as a lap warmer and study partner but have since crossed the rainbow bridge. Their comfort will be missed!

TABLE OF CONTENTS

TABLE OF CONTENTS CONTINUED

LIST OF TABLES

Table Page

LIST OF FIGURES

Figure Page

ABSTRACT

The degradation of riparian systems due to the influence of human activity has had a significant impact on biotic assemblages commonly found in these unique zones around the world. The regulation of waterways via damming and withdrawal is one example of how human activity has altered river hydrology leading to adverse ecological impacts on riparian structure and function. Riparian structure and function are constrained by many factors including, among others, a natural flow regime to sustain biotic assemblages throughout a river's reach. A natural flow regime includes seasonal variations in water inputs as well as changes brought about by disturbance events, such as floods. Therefore, my study will aim to highlight a high water event and the subsequent water recession directly related to the recruitment of many early successional species commonly found in riparian areas, specifically the *Populus* species. The study area will focus on a 24-km regulated segment of the Red River, bordering Oklahoma and Texas. Given my area of interest, only the eastern cottonwood (*Populus deltoides*) will be considered in the analysis. A novel methodology relying on remotely sensed data, specifically synthetic aperture radar data, is presented here. My methodology was able to isolate the water surface extents from the chosen high water event while quantifying the corresponding recession rates over a period of 36 days. A spatially explicit map corresponding to the favorability of *Populus deltoides* recruitment was produced according to a strict interpretation of established thresholds. I subdivided the 24-km reach of the Red River into 23 1-km segments to increase computational efficiency whereby 5 segments resulted in being classified as a marginal cottonwood recruitment areas and 1 segment classified as being favorable for cottonwood recruitment. My results from this study suggest the method performed very well given the chosen disturbance event was marginal at best for cottonwood recruitment. Continued refinement in the methodology to improve performance as well as addressing uncertainty in the data will need to be explored further to produce a model appropriate for cottonwood recruitment.

INTRODUCTION

Riparian Structure and Function

Riparian systems form at the boundaries of freshwater and terrestrial systems, and are characterized by a wetness gradient from the surface water to the upland area. The diversity of biotic and abiotic elements as well as ecological processes present in this wet-dry interface are constrained by topographical positions, climatic drivers, disturbance regimes, and land-cover patterns. Hydrologic dynamics such as precipitation, groundwater return flows, and the resulting flow regime and flashiness of a river also shape the extent and integrity of riparian systems. Landscape-scale topography and soil composition influence these hydrogeological processes, and therefore are an additional influence on riparian characteristics. Among these many influences, topographical position in relation to the water surface and the hyporheic water table is the primary constraint on the presence, extent, and diversity of riparian biotic assemblages.

Vegetation common to riparian areas includes patches of woody species forming stands of various ages. Riparian forests form along the soil moisture gradient within the wet-dry interface, and this gradient is a significant constraint on the presence and arrangement of woody species. Recruitment and successional stages of riparian vegetation are also influenced by a river's disturbance regime, including low flow events and flood events producing high stage elevations. The frequency of high flow events can alter the ecological structure of a riparian area, thereby impacting community structure and ecological processes. For example, a high flow event is likely to result in the denudation of stream bank vegetation thereby leading to the colonization of early successional species. Riparian forests that are shaped by the hydrology and disturbance regimes of rivers perform important ecological functions, including mitigating sediment loading

to river systems, stabilizing stream banks to increase reach resiliency in response to disturbance, providing wildlife habitat, controlling water quality by intercepting excessive nutrients derived from upland sources, introducing organic material to support lotic trophic webs, and providing protection from extreme water temperature changes by producing shade thereby creating thermal refugia for aquatic fauna.

Populus Physiology and Phenology

Populus spp., commonly known as cottonwoods, are a common woody species present in healthy riparian systems and are dependent on a natural disturbance regime. The cottonwood nomenclature generally refers to a group of three *Populus* species belonging to either the *Aigeiros* subsection or *Tacahamaca* subsection of the genus (Mahoney and Rood, 1998). The *Aigeiros* subsection is made up of the eastern cottonwood (*Populus deltoides*) and is characterized as a broadleaf cottonwood found throughout the contiguous United States. The *Tacahamca* subsection includes the black cottonwood (*Populus balsamifera* ssp. *trichocarpa*) and the narrowleaf cottonwood (*Populus balsamifera* ssp. *angustifiola*) and are characterized by having a lanceolate leaf structure found in parts of the western United States.

Cottonwoods are early successional riparian species populating barren areas of streambanks where soil moisture and hyporheic flow are critical elements to their survival. The ecophysiology of cottonwoods can be best described as phreatic, indicating their dependence on the proximity of the hyporheic capillary fringe to sustain the growth of the plant. Cottonwoods have a prolific growth rate and provide many ecological benefits as young cottonwoods have the potential to add 1 to 2 m of new growth per year in ideal landscape positions. For example, the vertical growth and canopy extent can provide cover to wildlife moving through the riparian

corridor to escape weather events (i.e., high temperatures, rain events, etc.), provide food for browsing animals, and partial shade to lotic systems resulting in cooler patches for aquatic fauna to escape warmer waters. For developed riparian areas, the ecological benefit of cottonwood patches preserves areas utilized by people for recreational use by maintaining water quality for fishing, providing significant shade and cover for parks, and habitat for wildlife viewing. While the cottonwoods' ecological value is significant, the species is generally short-lived in a natural setting as frequent disturbances from biotic and abiotic influences are significant stressors that can lead to premature death. Moreover, cottonwoods have a low-density physical structure indicating that the wood is soft and prone to breakage. Thus, when exposed to disease or damage due to insect presence and/or a natural disturbance (i.e. aeolian, flood), the felling of individual trees is likely to occur. Due to their short-lived nature, cottonwood populations are intricately dependent on seed development, dispersal, and germination as well as the presence of specific ecological conditions for successful recruitment and replenishment on a periodic basis (Braatne et al. 1996).

Cottonwood seed dispersal phenology is a critical component to successful recruitment within a riparian landscape. The timing of seed dispersal is largely dependent upon latitudinal position with lower latitudinal positions producing the characteristic cotton-like fluff during the spring months. For example, cottonwood stands between 30° and 35° north latitude positions have a mean seed dispersal beginning on or around May 1 of each year (Rood and Kaluthoda, 2020). However, seed dispersal can last for up to two or three months depending on which species and where the individual tree sits within the landscape (Mahoney and Rood, 1998). Cottonwoods are prolific seed producers reaching millions of seeds produced by a single tree in a

single season. The seed structure is characterized as a small green pod attached with light feathery spindles maximizing wind-aided or anemochory dispersal. Depending on the wind regime of a particular landscape position, cottonwood seeds can be dispersed over a few hundred meters with the possibility of dispersing over longer distances (Braatne et al. 1996). In addition to anemochoric dispersal, cottonwood seeds that have fluttered onto water surfaces use the streamflow or hydrochlory dispersal strategy whereby a high-flow stream condition can transport seed pods downstream and deposit them onto riparian positions as the water recedes. Cottonwood seeds germinate within 7 days of dispersal, and generally require barren, moist riparian positions with access to the water table to facilitate their survival and growth. A vast majority of cottonwood seedlings are likely to perish due to desiccation in dry upland positions or when soil moisture recession rates are too high, or to a lesser degree scour from a fall season high flow event (Rood et al., 2003; Benjankar et al. 2014).

Hydrological Considerations for Cottonwood Recruitment

With natural cottonwood recruitment effectively compromised due to regulated systems, it is necessary to identify suitable locations with intact ecohydrological processes that can partially support the re-establishment of cottonwood stands in riparian areas. Periodic functional or environmental flows (controlled dam release) may be beneficial in reestablishing some riparian cottonwood stands in some areas but decisions regarding flow release rarely consider cottonwood recruitment (Foster et al., 2018). For regulated systems without controlled releases, a storm event of specific magnitude to produce localized flooding may allow for isolated areas of cottonwood recruitment. The recruitment of cottonwoods is constrained by many ecological

variables and each explanatory variable can in part be analyzed to derive potential riparian landscape recruitment positions (Figure 1).

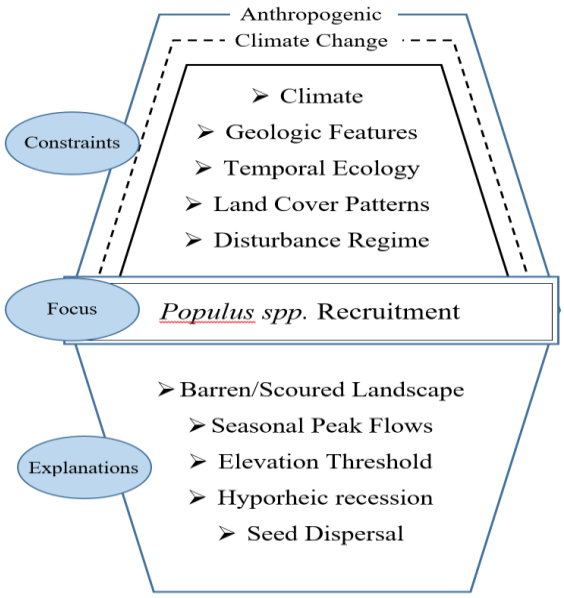

Figure 1. Conceptual Model adapted from the Hierarchal Theory from O'Neill et al. (1986).

Identification of areas potentially suitable for cottonwood recruitment within a regulated riparian corridor can be evaluated against established ecohydrological metrics proposed in the recruitment box model by Mahoney and Rood (1998). The recruitment box model is a graphical representation describing the various ecohydrological elements needed for successful cottonwood recruitment (Figure 2). There are three essential elements to forming the "box" that must be considered: timing of seed release, stream stage above baseflow, and stream stage decline after a disturbance. Of the three essential elements, a disturbance of sufficient magnitude

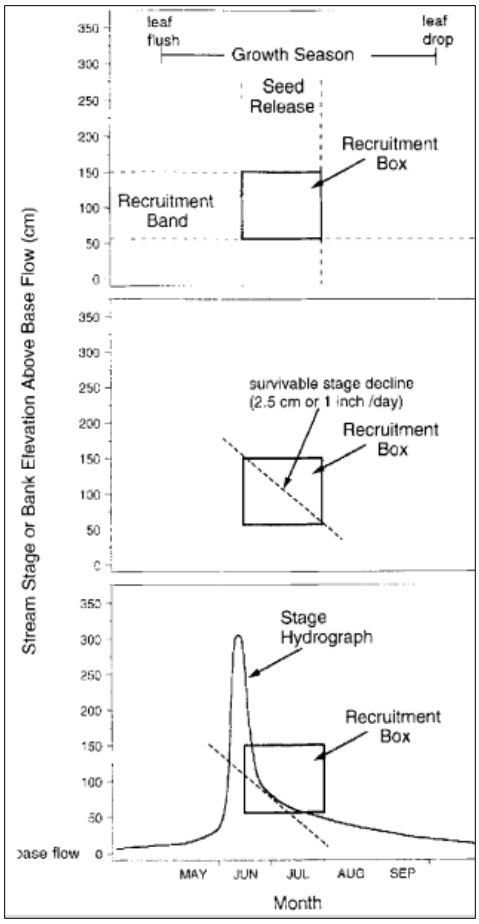

Figure 2. Recruitment Box Model
Source: Mahoney and Rood (1998)

is required to create conditions favorable for cottonwood recruitment. Variability exists in contemporary literature regarding the magnitude of disturbance, however Mahoney and Rood (1998) suggest a high flow event with a recurrence interval (RI) between a 5-yr and a 10-yr event creates the most favorable conditions for successful cottonwood recruitment. Foster et al. (2018) suggest a weighted range of disturbance events starting with a 20-yr or higher RI event within a 2 year period to the lowest weighted events below a 5-year RI are possibilities related to cottonwood recruitment.

In large part, regulated flow regimes of lotic systems are responsible for interfering with natural cottonwood recruitment processes within riparian areas. With many river systems

influenced by human activity due to increased demand for water resources, cottonwood stands are slowly declining in parts of the United States. The flow regime of streams or rivers are determined largely by geographic variation in landscape constraints (Figure 1) resulting in variability in peak flows that normally occur during the spring from snowmelt or seasonal wet weather, as well as during low flow or baseflow conditions during hot, dry seasons (Poff et al., 1997). However, for regulated river systems whereby tributaries and main stem river segments are dammed or diverted for human activity, flow regimes are fundamentally altered with the reduction of peak flows during seasonally wet weather patterns and increased flows during hot, dry months.

Cottonwoods are phreatic species where the process of root elongation for a seedling must, at a minimum, coincide with the receding hyporheic capillary fringe, otherwise, mortality is likely to occur due to desiccation. A natural disturbance regime will have periodic high flow events necessary to scour stream banks and provide the necessary water table recession rate for cottonwoods to be recruited. However, regulated systems often lose their natural peak flows as dams mitigate high flow events, which is a necessary component to create scouring along a stream bank. A river's hydrograph can illustrate the differences in flow patterns as well as determine recession metrics for successful cottonwood recruitment between regulated and non-regulated systems. A regulated river system often cannot sustain ecological functionality as less sediment is being conveyed for downstream alluvial deposition, and less scour is present to drive natural successional processes and subsequent cottonwood recruitment in riparian areas as suggested by the recruitment box model. The absence of a natural disturbance regime, the lack of

high-flow events, changes in hydrology, and competition from other species pose a challenge to effectively recruit riparian cottonwoods.

Study Objective and Goals

In light of the anthropogenic impacts as well as the specific ecohydrological conditions that must exist for cottonwood recruitment, I will use a synthetic aperture radar (SAR) data product to identify potential cottonwood recruitment areas within a riparian corridor with altered hydrology. SAR data products can be applied to a variety of ecological inquiries potentially impacting human interests, such as marine monitoring, land formations, and emergency services (ESA, 2022). As an example, SAR data products have been used extensively for flood mapping and the evaluation of flood related-impacts to human interests, such as potential damage to municipal infrastructure, are well established within contemporary literature.

My objective is to present a novel methodology using remotely sensed data, specifically SAR data, to broadly and rapidly predict areas of cottonwood recruitment. My presented methodology represents an initial workflow extending the SAR application to a specific ecohydrological phenomena by: (1) obtaining and analyzing a hydrograph with a suitable high flow event along a segment of the Red River of the South, (2) collecting and processing synthetic aperture radar (SAR) data products to identify water surface extents (WSEs) at multiple times during the recession following the high flow event, (3) quantifying the elevation bands from the boundary of all WSEs, and (4) presenting a spatially explicit map of potential cottonwood recruitment areas. The methods and findings presented here have the potential to assist vested policy-makers, managers, or others wishing to understand the spatial and temporal effects of anthropogenic and ecohydrological constraints associated with cottonwood recruitment.

STUDY AREA

Red River of the South

The Red River of the South, or the "Rio Rojo" as it was named by the Spanish explorers when encountering the distinctive red colored waterway in the 16th century, has a reach of over 2,070 km with the headwaters located in a small portion of West-Central New Mexico (Texas

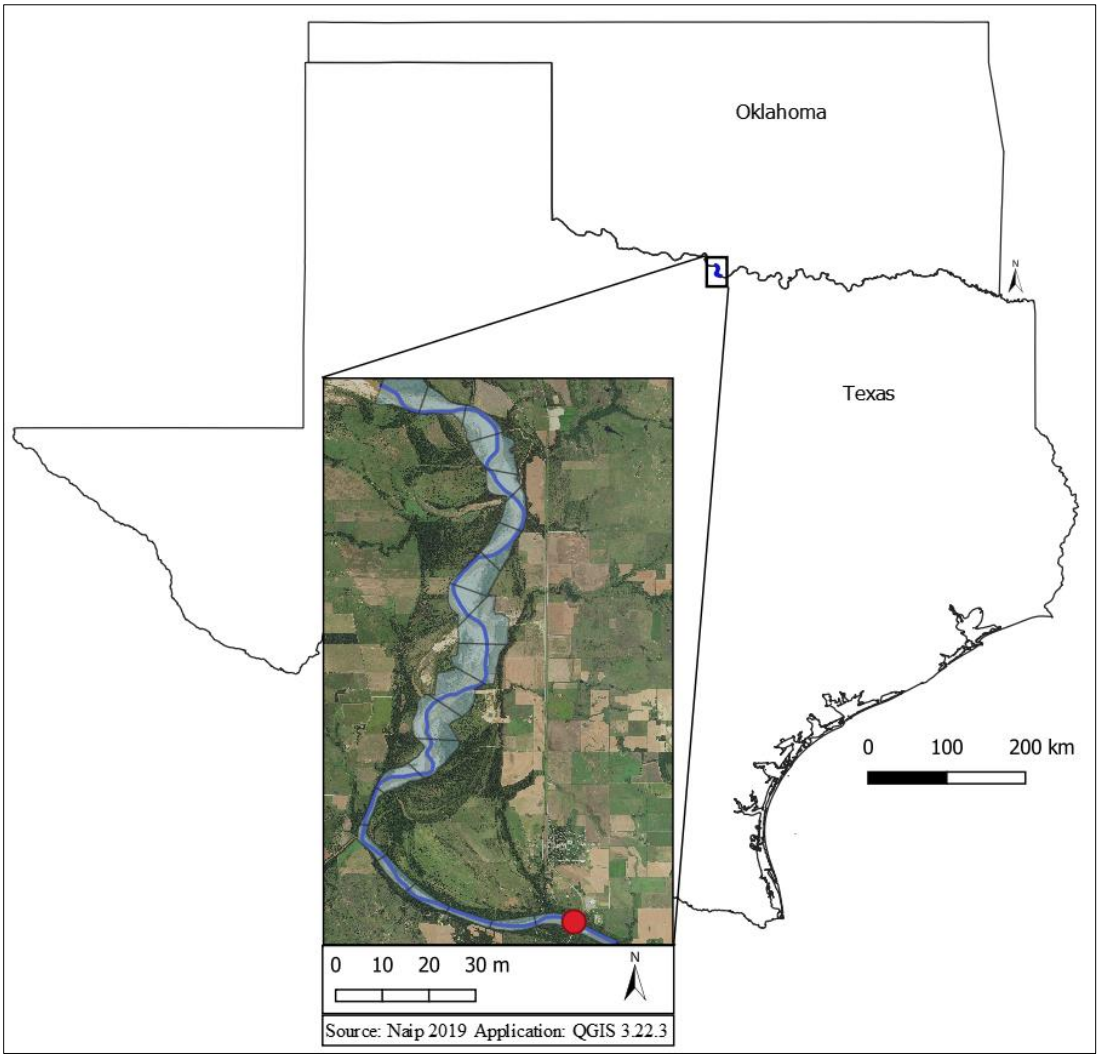

Figure 3. Red River Segment of Interest.

Almanac, 2022; Zamani Sabsi, 2019). The Red River is commonly known for being a contentious area between Oklahoma and Texas as the river forms the southern border of

Oklahoma or a portion of the northern border of Texas depending on individual perspective. The river flows primarily from west to east then veers to the southeast into Louisiana where the historical outlet is with the Mississippi River. However, the waterway now joins with the Atchafalaya River in Louisiana just west of the Mississippi River. The Atchafalaya River Basin is a distributary of the Mississippi River forming the largest riverine wetland in the United States (ANHA, 2022). I will focus on a 24-km regulated segment located on the Oklahoma-Texas border within a humid subtropical system (Figure 3). As the *Aigeiros* subsection (*Populus deltoides*) are the only cottonwood species present in the area (the *Tacahamaca* subsection varieties are absent), all references made to cottonwoods from this point forward will be limited to the *P. deltoides* species only.

Hydrogeology

The Red River basin has numerous tributaries with groundwater return flows that maintain baseflows within the main stem. The Red River can be characterized as being a responsive hydrologic system as precipitation events commonly result in floodplain intrusions. Regardless of the flow conditions, the water from the Red River has a unique coloration as runoff from upland iron-rich clays mix with the channel water producing a reddish-orange hue. The clay soils overlay mudstone and sandstones which together produce a near-constant turbid condition. Historically, the Western Interior Sea covered the area of interest and as the ancient sea waters slowly receded, large amounts of salts precipitated out from evaporation. Today, the salt deposits continue to be leached out via groundwater seeps contributing to the river's high salinity. During low flow conditions, the salinity of the Red River can reach levels equivalent to

sea water which influences many ecohydrological processes along the river's reach (Baldys and Phillips, 1997).

Hydrologic Data

The development of a cottonwood recruitment method hinges on identifying a suitable high flow event by evaluating hydrologic data from a nearby USGS gage station. Identification of the stage-height relationship of a high-flow event using USGS gage data coinciding with the timing of seed dispersal is a necessary step in the process. In addition to identifying and gathering stage-height data, recession rates will need to be calculated to determine if the rate of decline meets the recruitment threshold values established from a study by Burke et al. (2009). The hydrologic data are derived from USGS Gage 07315500 on the Red River near Terral, Oklahoma. The location of the USGS gage can be found at the lower end of the segment of interest between a railroad bridge and a vehicular bridge. The high flow event that occurred on May 27, 2019 and the subsequent recession will be the source-event for my study. My analysis will be limited to the riparian areas shaded light blue in Figure 4.

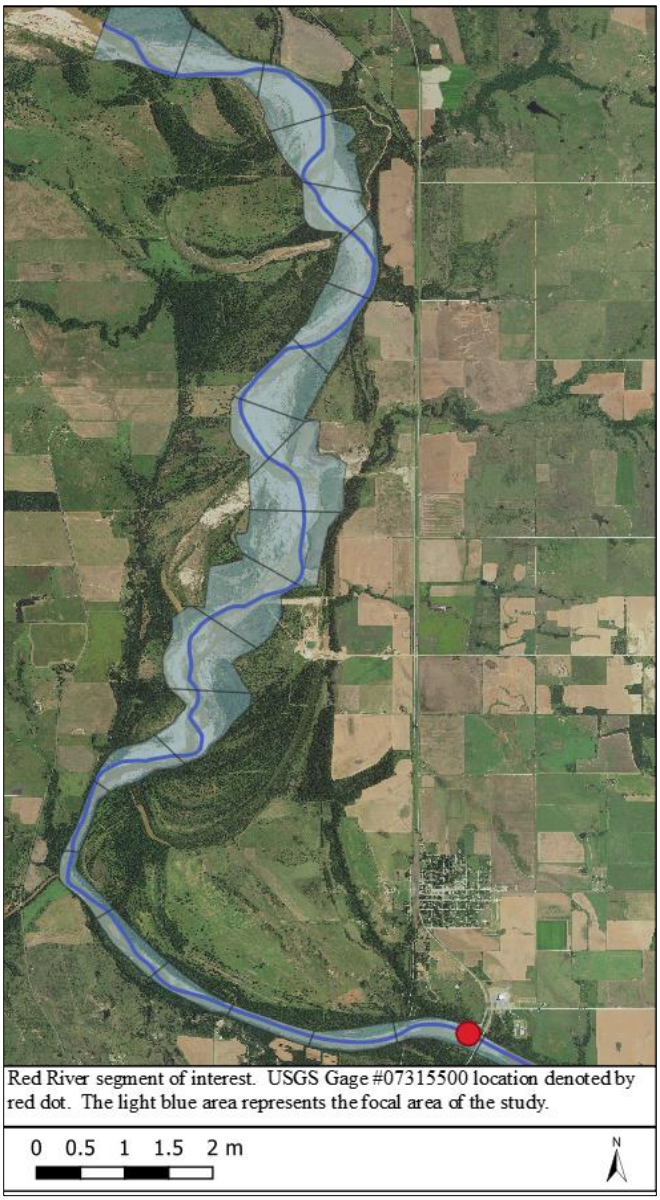

Figure 4. Riparian Area of Study

METHODS

Overview

I used remotely sensed data to determine water surface extents associated with the recession of a high water event. The water surface extents (WSEs) from the high water event were compared to a digital elevation model (DEM) and translated into an elevation band for the WSE boundary. A recession rate was then calculated from the WSE boundaries, and used to determine the suitability of cottonwood recruitment within the study area. The study area was segmented into 1 km regions to assist in the computational efficiency. Each segmented region of the study area was individually assessed for spatiotemporal cottonwood recruitment potential.

Remote Sensing Data Acquisition and Processing

The Sentinel-1 constellation data products were used to isolate the water surface extents from the high flow event that occurred on May 27, 2019. The Sentinel-1 constellation is comprised of two satellites (Sentinel-1A and Sentinel-1B) with a temporal resolution of six days or twelve days with one of the satellites. The instrument on the Sentinel-1 satellites performs C-band synthetic aperture radar (SAR) imaging (table 1) over four acquisition modes: StripMap (SM), Interferometric Wide Swath (IW), Extra Wide Swath (EW), and Wave. The IW

Table 1. Sentinel 1-A Specifications *Source: ESA, 2022*

Sentinel 1A Satellite	
Launch Date	April, 2014
Operating Agency	European Space Agency (ESA)
Sensor	Active Synthetic Aperture Radar – C Band
Orbit	Near-Polar Sun-Synchronous
Polarization	HH+HV, VV+VH, VV, HH
Repeat Cycle	12 days
Center Frequency	5.405 GHz
Radiometric Resolution	10-bit

acquisition mode is the most common imaging mode for terrestrial and fresh water observations (ESA, 2022). The IW mode is further delineated by two level-1 products, single look complex (SLC) and the ground range detected (GRD) products. IW-SLC pixel data include phased information with an in-phase (*i*) and quadrature (*q*) component with a slant range geometric extent, whereas the IW-GRD pixel information only contains an amplitude component (ESA, 2022). Phased pixel information is not suitable for conversion to a radiometric backscatter coefficient thus the IW-GRD product was selected for my study. Ground range detected IW-SAR products have been corrected using a process referred to as multi-looking. Multi-looking applications correct the slant range geometry commonly seen in single-look complex (SLC) IW-SAR products to an orthorectified extent. GRD SAR products will lose some fine-scale detail within the extent when the multi-look application is applied resulting in a slightly coarser spatial resolution (10 m) compared to the SLC SAR products (2.3 m x 14.1 m)

Unlike many optical sensors which are classified as passive sensors, the SAR instrument onboard the Sentinel-1 satellites are active sensors transmitting their own microwave (radar) radiation signal toward the Earth then recording the relative strength of the returned backscatter. The strength of backscatter returned to the SAR instrument is largely dependent on surface roughness. Rough surface features, such as vegetation, will return a relatively strong signal back to the sensor producing a bright area, whereas water features reflect the signal away from the sensor producing a very dark signal. The determination of water surface extents (WSE) and how far they intrude into and beyond the floodplain is a common SAR-processing technique for flood-mapping. However, the use of SAR data products in the evaluation of ecohydrological phenomena is somewhat limited within the literature. The novelty of my study is to present a

Table 2. SAR data files and naming conventions associated with the high-flow event that occurred along the Red River and is the focus of my study.

Cottonwood Recruitment SAR dataset			
Name	**Date**	**File Name**	**Polarization**
Image 1	May 27, 2019	S1A_IW_GRDH_1SDV_20190527T002742_20190527T002807_027406_031767_C59A	VH+VV
Image 2	June 8, 2019	S1A_IW_GRDH_1SDV_20190608T002743_20190608T002808_027581_031CC8_E8FC	VH+VV
Image 3	June 20, 2019	S1A_IW_GRDH_1SDV_20190620T002743_20190620T002808_027756_032208_16A7	VH+VV
Image 4	July 2, 2019	S1A_IW_GRDH_1SDV_20190702T002744_20190702T002809_027931_032749_D0D0	VH+VV

SAR-based workflow that moves beyond a simple WSE determination but rather isolates the WSE boundaries from a high-flow event over time and identifies the relative elevation of floodplain intrusion extent and corresponding recession. Critical metrics associated with cottonwood recruitment can then be quantified from a time-series analyses of a specific high-flow event.

Data Selection and Pre-Processing

The initial step is the selection of a SAR data set meeting the threshold values suggested from the Recruitment Box model presented in the article by Mahoney and Rood (1998), and Burke et al. (2009). Four data points (Table 2) were selected from the Sentinel-1A SAR sensor beginning with the data product from May 27, 2019 (image 1) as coinciding with the chosen high-flow event (Figure 5). The revisit time of the Sentinel-1A satellite for the area of interest is evenly spaced at twelve days between each pass (Table 1). The period of interest for my study spans 36 days from the initial peak labeled #1 in Figure 5 to near-baseflow conditions labeled #4. Once the selected data points (Table 2) had been established, corresponding Sentinel-1A GRD products were downloaded and held in a compressed file. I used the open-sourced Sentinel Application Platform (SNAP) version 8.0.9 program with the S1 toolbox (version 8.0.5) add on

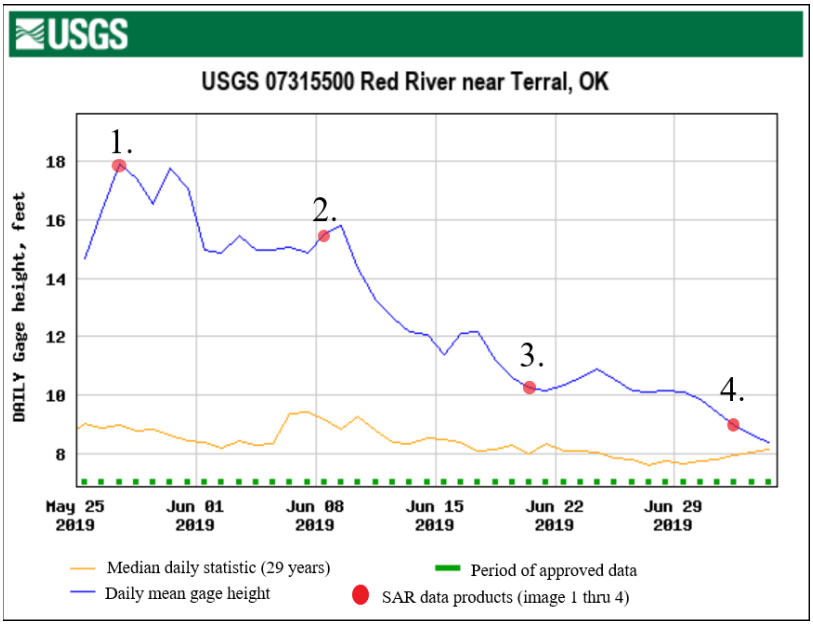

Figure 5. USGS Hydrograph with corresponding data product markers. Source: USGS, 2022

for processing the GRD products efficiently. With four GRD products corresponding to the dates indicated in Table 2, each product must be pre-processed independent of each other. Due to the operational mechanics of the SAR sensor, the initial impulse and the elapsed time of the subsequent backscatter return signal are not instantaneous thus resulting in a delay in the return signal back to the sensor. As the backscatter return signal is captured by the sensor, the satellite has traversed some distance away from its initial point of transmitting a radar impulse toward the Earth. Intuitively, the distance traveled by the sensor is dependent upon the velocity of the sensor but more importantly the position of the sensor relative to the angle of the return vector (return signal) is critical to producing an accurate SAR product. All GRD products generally have poor metadata as analysts must correct the metadata by applying an orbit file to account for the differences in satellite position and velocity. The orbit file is not immediately available after the data have been received. Analysts release the correct metadata in a separate file several days after the initial acquisition of data. Applying an orbit file to any SAR product is viewed as a

critical processing step. Once the metadata have been corrected, analysts must contend with a significant amount of noise associated with the SAR images. Pre-processing is a necessary process to remove as much noise as possible without compromising the data of interest. Pre-processing the GRD images begins with removing the thermal noise associated with the data. By applying a thermal noise removal process for each image, a normalization of the backscatter signal is made thus removing any discontinuities within the data (Filipponi, 2019).

The next step of the pre-processing requires the user to understand how the SAR signal is specifically transmitted and received. I acquired SAR data from the IW mode which results in a dual-polarized product. In other words, the sensor transmitted the radar signal in a vertical mode and received the return signal in both the horizontal and vertical positions, simplified as VH and VV, respectively. The best practices for the study of water surface extents using SAR data suggests the use of co-polarized products for mapping areas of inundation as opposed to the cross-polarized products (Sipelgas, 2021). The co-polarized products refer to the manner of signal transmission and reception which includes the vertical transmit and the vertical receive data products, or the horizontal transmit and horizontal receive data products, referred simply as a VV or HH product. I chose the VV product for my analysis. Each VV product was isolated and processed out of the dual polarized product (VV and VH). Separating the data product from a dual polarized product (VV and VH) to a single polarized product (VV product) can be done by applying the border noise removal tool in the SNAP program. The border noise removal tool essentially corrects the image edges by removing any erroneous data points as well as removing radiometric artefacts associated with azimuth and range corrections (Elizavetin, 2010). Radiometric artefacts result from ambiguities within the return signal strength due atmospheric

variations between the sensor and the terrain object as well as changes to the sensor position. An illustration detailing the geometries associated with the SAR signal, including range and azimuth, can be reviewed in Figure 14 (Appendix A).

Backscatter Calibration

With the noise removal pre-processing complete, the pixel values must be calibrated and converted to a radiometric SAR backscatter. The radiometric SAR backscatter is commonly referred to as the backscatter coefficient or sigma naught (σ^o). For simplification, sigma naught represents a measure of the radar signal strength reflected by a physical feature on earth forming a normalized dimensionless unit (ESA, 2022). Sigma naught images are essential in the analyses of ecohydrological phenomena as terrestrial features will generally give relatively high values and values for surface water will be close to zero. A commonly observed pattern of backscatter strength relates to the surface roughness of physical features where greater surface roughness of a physical object will produce higher sigma naught values compared to objects with relatively smooth surfaces. For example, trees and shrubs have a high sigma naught value and will appear as bright pixels within the image extent. In contrast, roads and parking lots have a lower sigma naught value with relatively smooth surfaces and appear as a greyed pixel. Water completely reflects the radar signal away from the sensor resulting in a value close to 0 and will appear as a dark pixel. Derivation of a sigma naught image requires the pre-processed VV product be calibrated using the S1 toolbox for the SNAP application. The calibration procedure converts the pre-processed data products into a sigma naught extent with each pixel representing the relative strength of backscatter at a spatial resolution of 10 m. The sigma naught extent is very

likely to contain granular noise or a speckling of pixels within the extent and is likely due to conditions resulting in changes in backscatter signal (Figure 6– left image).

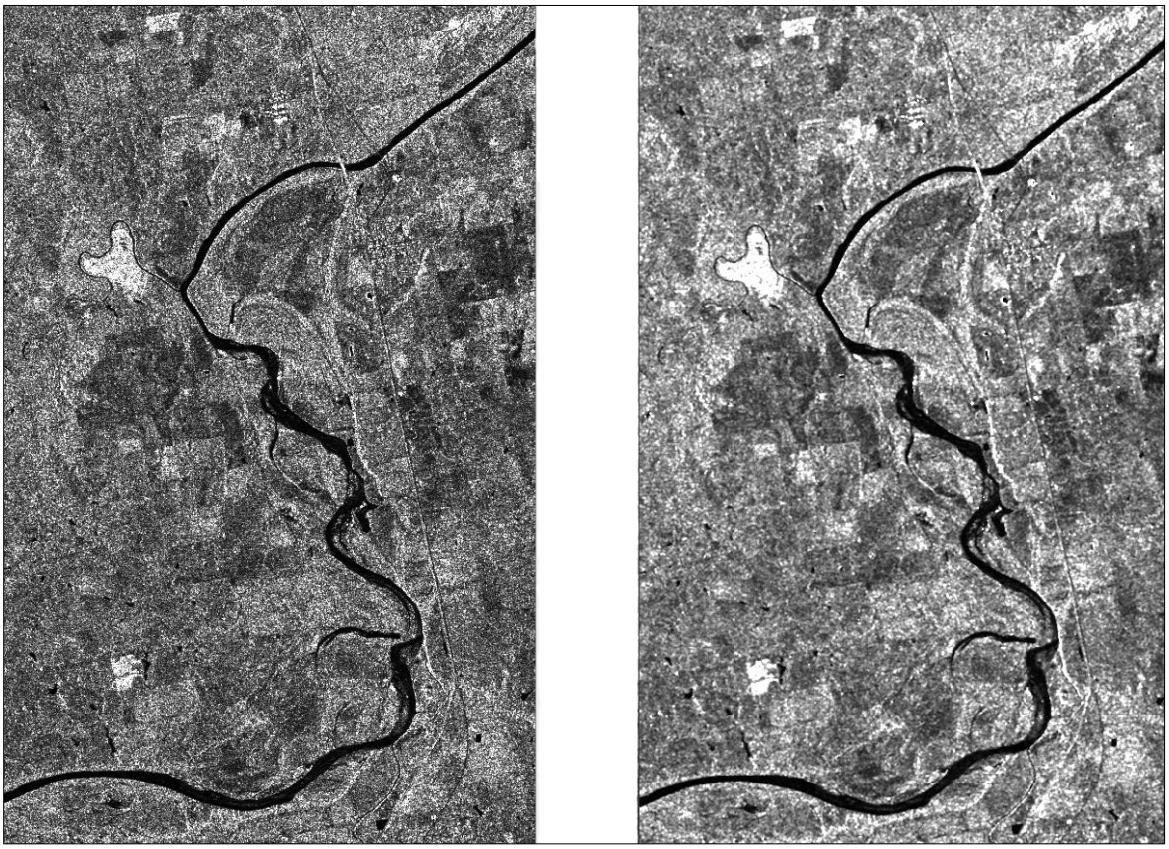

Figure 6. (left) raw Sigma Naught extent from 6/8/2019, (right) Lee-sigma filtered Sigma Naught extent from 6/8/2019.

Lee et al. (1994) discuss the mechanisms related to sigma naught processing and the associated pixilation of the extent by indicating that small changes in the surface roughness within the resolution cell are likely to result in variations within the signal strength thus leading to a speckling effect. Many speckle filters exist to suppress the magnitude of speckling from the extent, but caution is warranted as filtering can cause a loss of fine spatial details within the extent. Speckle filters operate by smoothing the signal intensity of a pixel by evaluating neighboring pixels to produce a more consistent representation. User inputs largely determine the magnitude of filtering as filters can be manipulated to extend well beyond a given pixel. I

chose the Lee-Sigma speckle filter with the lowest possible inputs as it appears to preserve much of the linear and textured information related to water surface extents (Figure 6– right image). Users are encouraged to use a filter that best meets their needs relative to their geospatial inquiry.

Data Post-Processing

After the pre-processing noise removal and the generation of a speckle-free sigma naught extent, the extent must be projected correctly for the area of interest. Sigma naught extents must be correctly oriented and projected as accurately as possible by applying a terrain correction to the data. The pre-processed extents are oriented with the swath path of the S1A satellite and are upside down relative to the correct orientation. Using the S1 toolbox for the SNAP program can

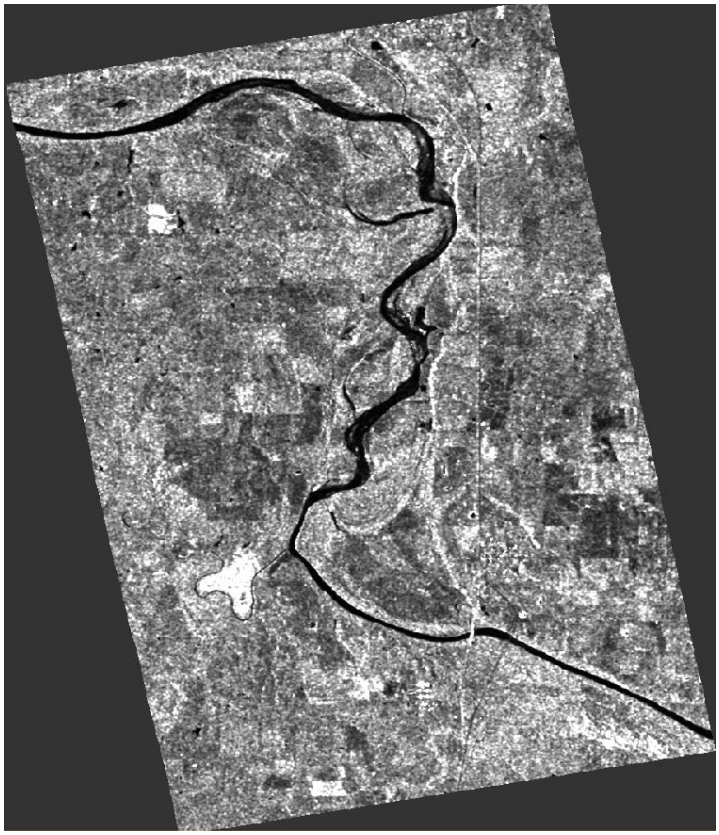

Figure 7. Terrain corrected (processed) sigma naught extent from 6/8/2019

streamline the process whereby range doppler terrain correction is applied. Aside from correcting the orientation and projection, range doppler terrain correction intends to correct some of the distortions associated with the side-look geometry commonly found with SAR data analyses, including effects of foreshortening, layover and shadows, by applying a digital elevation model to correct the location of the pixels (Filipponi, 2019; Brown and Hogan, 2020). The geometric distortions caused by foreshortening, layover, and shadowing (Figure 15 – Appendix A) are more pronounced in montane landscapes but still must addressed when using GRD SAR images. Users may select an auto download of a 30-m or 10-m digital elevation model (DEM), or use an external DEM during the application of the range doppler terrain correction. The 30-m DEM is sufficient to correct the geometric distortions associated with a sigma naught data product and was applied to each terrain corrected sigma naught image (Figure 7).

Only the WSEs are needed from the sigma naught extent as the terrestrial features lend no value to my analyses. Similar to a land-use/land-cover classification scheme, a histogram analysis of the backscatter coefficient distribution can be used to distinguish between areas that are water versus areas with a very smooth surface and appear as water. Physical features that are very smooth will be dark in a sigma naught extent but can be distinguished from pixels that are water by analyzing the sigma naught histogram. Extracting the WSE using the histogram analysis was performed manually for each image to reasonably identify water surface boundaries (Figure 8). The manual process for extracting the WSE was the same for each of the four SAR images. Each histogram from each terrain-corrected sigma naught extent was transformed via a decibel conversion (Figure 8). The objective behind transforming the distribution allows for a

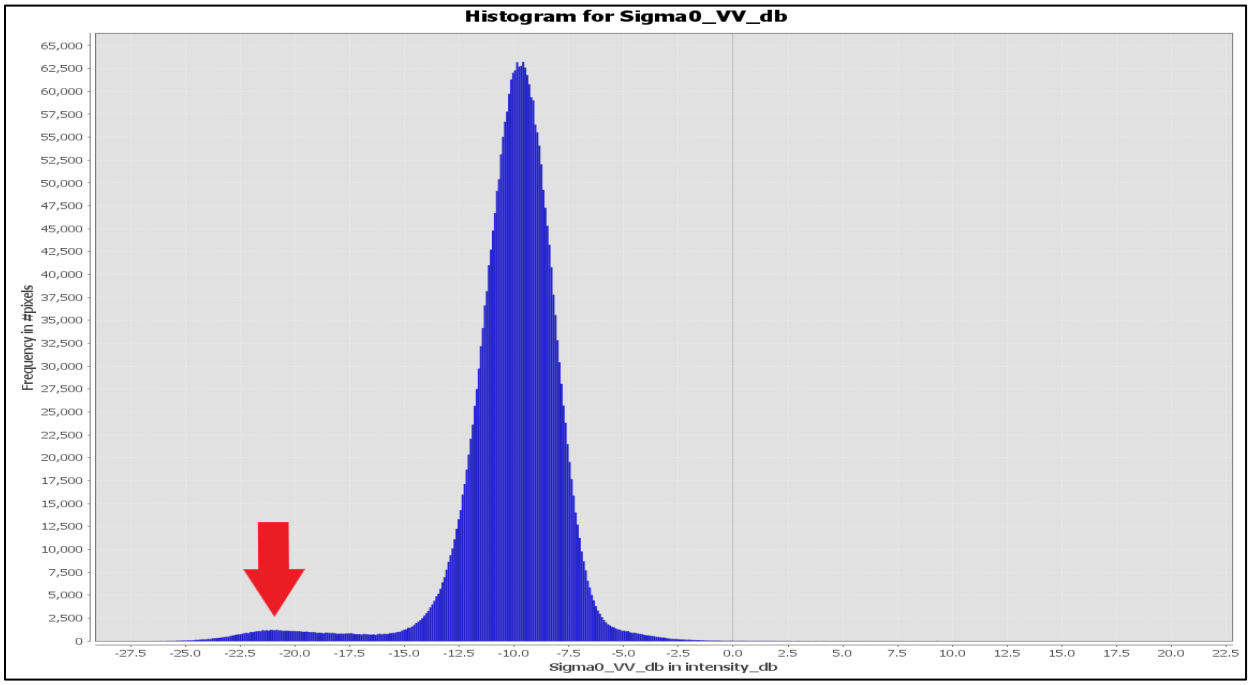

Figure 8. Histogram from the 6/8/2019 (Image 2) sigma naught extent that has been transformed to view the peaks. Water is represented by the very small peak to the left of the large peak (red arrow). Application: SNAP 8.0.9

user to readily identify the two peaks within the distribution and establish a necessary threshold between the water extent and terrestrial features (Long et al. 2014). The first peak (very small) in Figure 8 (red arrow) represents values associated with water, whereas the larger second peak represents all the upland features in the landscape. The slight valley between the first and second peak is selected as the demarcation area and the range of values from zero to the demarcation area (Table 3) represents all the pixels associated with water. Using the band math application (similar to a raster calculator in GIS programs) within the SNAP program, the water surface extent for each of the four images were extracted and exported into a GEOTIFF file.

Table 3. Histogram Analysis.
Demarcation values for each image

Histogram Analysis: Decibel transformation values		
File	**Date**	**dB**
image 1	5/27/2019	-15.38
image 2	6/8/2019	-15.85
image 3	6/20/2019	-16.15
image 4	7/2/2019	-16.43

Elevation and Recession

Predicting cottonwood recruitment potential for a given geographical point requires a quantitative understanding of elevation along the boundary of a WSE. Predicting recruitment locations along the segment of interest requires the demarcation of an elevation band associated with the boundaries of each WSE. A digital elevation model (DEM) was used to translate the WSE boundary data into a corresponding set of elevation bands. Due to the sigma naught data products having a 10-m spatial resolution, a 10-m DEM was chosen to optimize the precision and efficiency of the process.

Recession Rate

Again, the recession rate is a critical metric that needs to be quantified to reasonably predict cottonwood recruitment areas at the reach-scale. A temporal analysis of the WSE boundary elevation bands was performed to derive the water surface recession rate. Before calculating recession rates, the four sigma naught images of the reach (image 1 – 4) were divided into 1 km segments using the voronoi polygons command within the R statistical software (R Studio Team, 2022). Each of the resulting voronoi polygons, or reach segments, represent the area associated with a series of points placed at 1 km intervals along the reach beginning at the

0.5-km point (Figure 9). The segment numbers presented in Figure 9 were generated by the voronoi polygon application and do not correspond to any meaningful sequential order. The

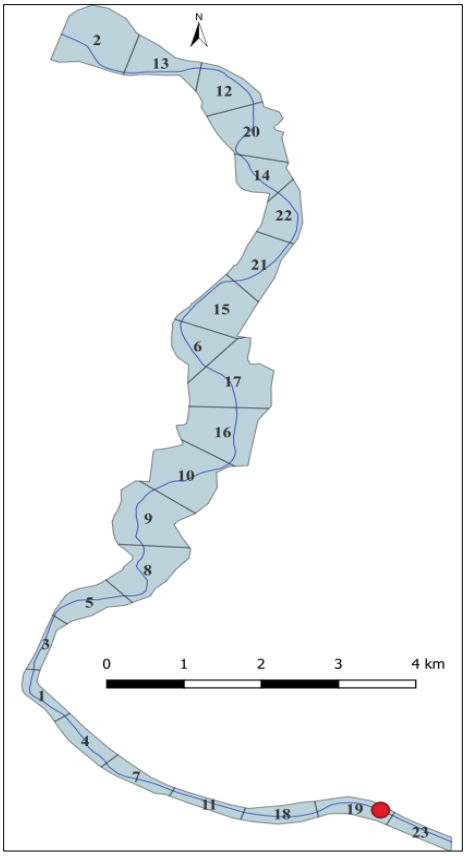

Figure 9. Voronoi polygons.

rationale behind using the voronoi polygons to segment the entire extent is twofold. First, a river's reach of 24 km will not have the same elevations at the upper and lower ends. To account for the slope of the river, the reach must be divided in a manner so the river slope within each segment is reasonable, and therefore the elevation bands for the WSE boundaries are meaningful. Second, processing of the elevation band that coincides with the boundaries of the WSE can be taxing to a computer as the dataset could include thousands of data points. By dividing the reach into segments, this ensures processing can be performed without expensive computer hardware and results in efficient and timely processing taking minutes rather than hours to complete.

To maximize the speed of processing and identify the elevation bands associated with the WSE for each image, R-studio was used to automate the task of identifying the elevation bands. (R Studio Team, 2022). However, a couple of parameters must be analyzed and used as inputs

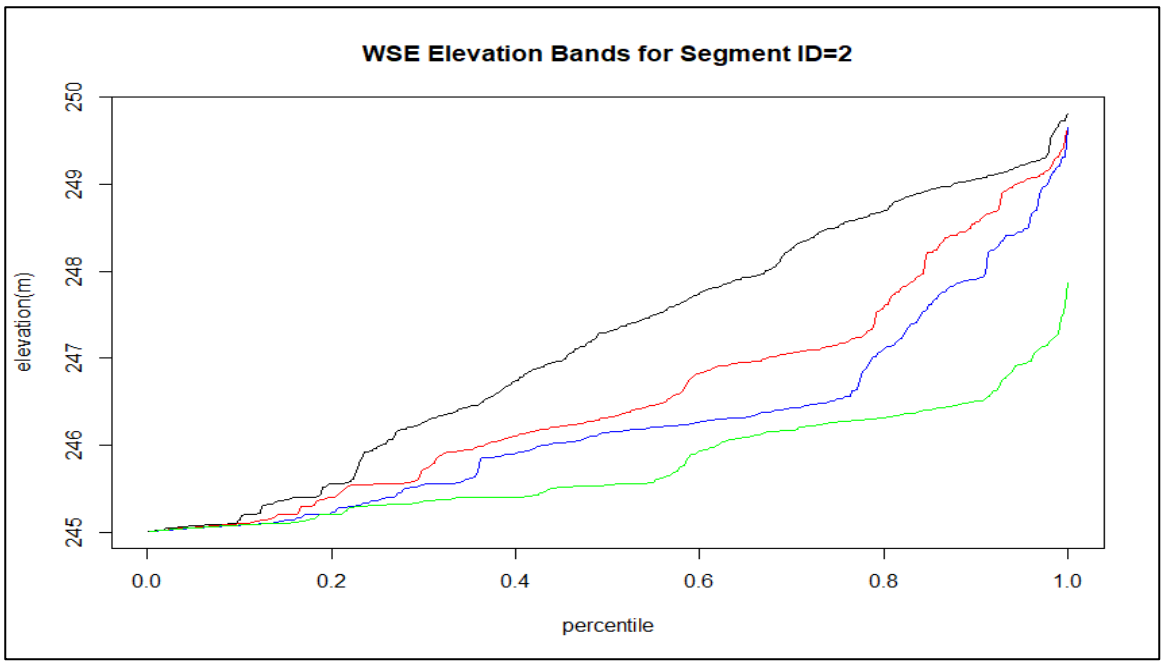

Figure 10. Water Surface Extent (WSE) Elevation Bands for Segment #2. Black line represents May 27, 2019 (image 1) data, red line represents June 8,2019 (image 2) data, blue line represents June 20, 2019 (image 3) data, and the green line represents July 2, 2019 (image 4) data.

before running the R-script. First, an analysis of the distribution of elevation values for each WSE boundary characteristic of a receding water surface boundary after a high flow event must be performed (Figure 10). In addition, each image within the temporal series (Figure 10 – different colored lines) should show an overall reduction in elevation values as the WSE from a high-flow event recedes over time. Manually evaluating every segment to ensure the plots illustrate a change in slope as well as temporal evaluation of showing a decrease in WSE boundary elevation data points is necessary before proceeding further.

With a focus on delineating the boundaries of a WSE and assigning a single elevation value for the entire band, each segment and from each image is subjected to a quantile method

(Cian et al., 2018a, b). Cian et al. (2018a) presented a quantitative methodology by collecting the distribution of elevation values that fell along the WSE boundary. The WSE boundary elevation distribution was then partitioned based upon a quantile method. The authors derived an elevation value for the WSE boundary by beginning at the 0.95 quantile and stepped downward 0.05 until the change was minimal. Once the change met the minimal threshold (≤ 10 cm) established, the elevation value at the n^{th} step was selected for the entire WSE boundary (*n* represents the number of steps taken). The quantile method from Cian et al. (2018a) generally showed 0.85 percentile to be a sufficient elevation value to assign to the WSE extent. The rationale behind the quantile method is that a simple, reproducible methodology for selecting a single data point from a range of raw elevation data to represent the entire elevation band is feasible.

While feasible, the quantile methodology must account for possible erroneous data points (i.e., outliers) and processing errors (i.e., filtered SAR images) for the method to perform as expected. I chose a conservative quantile of 0.7 and was used for most of the reach segments as the elevation values from the WSE boundary (equation 1.1) showed a minimal change and the WSE showed a general recession (Figure 10).

$$E_{WSE(s)} = E_{P(n)} - E_{P(n-i)} \qquad \text{(Equation 1.1)}$$

Where $E_{WSE(s)}$ refers to the derived elevation value for the WSE boundary for each SAR image *s*, *P* is the elevation value at *n* quantile percent, and *i* is the number of quantile percentage steps away from *n*. To ensure the quality of the calculated WSE elevation band ($E_{WSE(s)}$) was reasonable, each individual segment elevation band was plotted and manually interpreted to align with the recession of the actual WSE (calculated from USGS gage data) and demonstrated a

reasonable decline in the elevation of the WSE extent over the temporal series (4 images). There were a few segments for which the standard quantile value of 0.7 was not appropriate. For these segments, alternate values were manually determined after interpreting the range of data between all 4 images (Table 4). The quantiles were sourced in the R-script and required for the process to be automated.

Table 4. Calculated Quantiles for each segment.

Segment Numbers	Quantile Coefficient
1	0.7
2	0.7
3	0.7
4	0.7
5	0.7
6	0.7
7	0.7
8	0.7
9	0.5
10	0.7
11	0.7
12	0.77
13	0.77
14	0.25
15	0.7
16	0.335
17	0.65
18	0.7
19	0.7
20	0.175
21	0.7
22	0.39
23	0.7

A key metric for my study is the establishment of recession rate threshold values and corresponding cottonwood recruitment potential categories. Contemporary literature shows consistency in describing the recession rates belonging to three to five categories of cottonwood recruitment potential (Braatne et al., 2007; Burke et al., 2009; Benjankar et al., 2014; Benjankar et al., 2020). For simplicity, my study used three categories for the range of recession rate values

(Table 5). Once all the inputs and categories had been set, the R-script could quantify the elevation bands for the WSE boundary and recession rates for each recession image extent and

Table 5. Categories of recruitment potential and corresponding thresholds.

CW Recruitment Potential	Recession Rate (cm/d)
Lethal	>10.0 or <0.5
Marginal	10.0 to 5.0
Favorable	<5.0 to 0.5

for each segment. Each recession extent (RE_n) can be calculated as the elevation band change for each WSE boundary ($E_{WSE(s)}$) divided by the number of days elapsed (d) between images. To align with the recession rates established in the literature, the recession extent is multiplied by 100 to return a value in cm per day. With four images in the dataset and $E_{WSE(1)}$ representing the peak of the high-flow event, three recession rate extents were calculated based on the following equations:

$$RE_1\ (cm/d) = \left(\frac{E_{WSE(1)} - E_{WSE(2)}}{d}\right) * 100 \qquad \text{(Equation 1.2)}$$

$$RE_2\ (cm/d) = \left(\frac{E_{WSE(2)} - E_{WSE(3)}}{d}\right) * 100 \qquad \text{(Equation 1.3)}$$

$$RE_3\ (cm/d) = \left(\frac{E_{WSE(3)} - E_{WSE(4)}}{d}\right) * 100 \qquad \text{(Equation 1.4)}$$

Where RE_n represents the recession extent and the calculated recession rate value and d is the number of days elapsed between the two images. The recession rates for each segment

throughout the recession extent were strictly interpreted on an individual and sequential basis based on the assigned threshold values (Table 5).

Geospatial Information System (GIS) Application

Quantifying areas of WSE recession that align with established metrics and thresholds available from existing research is an essential procedural step to identify potential cottonwood recruitment areas. For the recruitment method to rapidly disseminate data tables related to cottonwood recruitment potential, a thematic map must be produced. As such, the elevation bands for the WSE boundaries, the recession rates for each extent, broken down by segment, and the categories of recruitment potential can be easily produced in a data table and subsequently attached to the attribute table of the vector recession extents (RE_n). The recession extents are derived from the difference between the sigma naught images. For example, the first recession extent (RE_1) can be mapped by taking the difference between image 1 and 2. Mapping out recession extents can be readily performed by any GIS application. Mapping of the recession extents with the associated recession data tables attached was performed using QGIS 3.22.3.

RESULTS

Data Analysis

With the reach divided into 23 segments as described above, the elevation band for each segment corresponding to the WSE boundary is recorded for each SAR product (image 1 – 4) (Table 6). Each recession rate for each segment was calculated using equations 1.2-1.4 and the corresponding classification of the recession rate (cm/d) was performed (Table 6). The last data column refers to the overall favorability of a recession rate being classified for potential cottonwood recruitment (Table 6). Classifying the overall recruitment potential must evaluate each recession rate value (cm/d) in succession and applying the categorical threshold to the recession rate value. For each segment, if a lethal category had been determined by the model

Table 6. Favorability of cottonwood recruitment for each analyzed river segment, and each timestep.

	Elevation Band for WSE boundaries				Recession #1 Extent		Recession #2 Extent		Recession #3 Extent		Overall CW Recruitment Potential
Segment Number	Image 1 (m)	Image 2 (m)	image 3 (m)	image 4 (m)	Recession Rate (cm/d)	CW Recruitment Potential	Recession Rate (cm/d)	CW Recruitment Potential	Recession Rate (cm/d)	CW Recruitment Potential	
1	238.6	238.6	238.5	238.6	0.0	lethal	0.8	favorable	-0.8	lethal	lethal
2	248.3	247.1	246.4	246.2	10.0	marginal	5.8	marginal	1.7	favorable	marginal
3	239	239	239	239	0.0	lethal	0.0	lethal	0.0	lethal	lethal
4	238.7	238.5	238.5	238.6	1.7	favorable	0.0	lethal	-0.8	lethal	lethal
5	241.6	240.4	240.6	240.6	10.0	marginal	-1.7	lethal	0.0	lethal	lethal
6	245.4	245.4	246	246.2	0.0	lethal	-5.0	lethal	-1.7	lethal	lethal
7	239.1	239	238.7	238.7	0.8	favorable	2.5	favorable	0.0	lethal	lethal
8	242.7	241.7	241.7	241.6	8.3	marginal	0.0	lethal	0.8	favorable	lethal
9	242.4	241.9	241.8	241.8	4.2	favorable	0.8	favorable	0.0	lethal	lethal
10	243.4	243	242.2	241.8	3.3	favorable	6.7	marginal	3.3	favorable	marginal
11	237.8	237.8	237.8	237.9	0.0	lethal	0.0	lethal	-0.8	lethal	lethal
12	246.9	246.2	246.3	246.1	5.8	marginal	-0.8	lethal	1.7	favorable	lethal
13	247.5	246.6	246.6	246.4	7.5	marginal	0.0	lethal	1.7	favorable	lethal
14	245.5	244.3	244.2	244.1	10.0	marginal	0.8	favorable	0.8	favorable	marginal
15	245.1	244.2	243.6	243.5	7.5	marginal	5.0	marginal	0.8	favorable	marginal
16	242.5	241.8	241.8	241.6	5.8	marginal	0.0	lethal	1.7	favorable	lethal
17	243.4	243.1	242.9	242.9	2.5	favorable	1.7	favorable	0.0	lethal	lethal
18	238.3	238.3	238.1	238	0.0	lethal	1.7	favorable	0.8	favorable	lethal
19	237.9	237.8	237.6	237.5	0.9	favorable	1.6	favorable	0.9	favorable	favorable
20	245.2	244	244.1	244.1	10.0	marginal	-0.8	lethal	0.0	lethal	lethal
21	244.8	244.2	243.6	243	5.0	marginal	5.0	marginal	5.0	marginal	marginal
22	244	243.2	243.3	243.3	6.7	marginal	-0.8	lethal	0.0	lethal	lethal
23	237.1	237.1	237.1	237.1	0.0	lethal	0.0	lethal	0.0	lethal	lethal

from any of the recession extents, then the overall category was determined to be lethal. If a recession extent was categorized as favorable in one of the three recession extents and the other two recession extents identified only marginal cottonwood recruitment potential, then the overall category was determined to be marginal. The only condition that would result in a favorable cottonwood recruitment area is if all three recession extents (RE_{1-3}) showed a favorable recession rate given the metric thresholds for each category (Table 5). For example, if the recession rate extent #1 (RE_1) is classified as lethal due to a high recession rate (> 10 cm/day), then the data from the recession rate extents #2 (RE_2) and #3 (RE_3) are likely to be irrelevant as the time elapsed between the first two extents is twelve days and is ample time to result in seedling desiccation.

According to the USGS 07315500 gage data, the high flow event I chose to study reached a peak discharge of 1,022 cubic meters per second (36,100 cubic feet per second) and a peak stage-height of 5.46 meters at the time of acquisition of the first SAR data product (image 1) on May 27, 2019 (Table 2). The discharge and stage-height values corresponding to the acquisition dates and times for each SAR data product are also provided (Table 7). The RI coinciding with the date of acquisition for each SAR data product was also calculated from the peak flow and stage height data provided by the USGS 07315500 hydrological record (Table 6). The period of record for the gage is robust while covering a span of 85 years beginning in 1935. Using the RI

Table 7. Hydrology of the Red River near Terral, Oklahoma. Source: USGS

USGS Gage 07315500 Hydrology. Red River near Terral, Oklahoma					
SAR data product	**Date**	**Discharge (Q), (cfs)**	**Stage-Height, (ft)**	**Stage-Height, (m)**	**Recurrence Interval (RI)**
Image 1	May 27,2019	36,100	17.93	5.46	1.84
Image 2	June 8, 2019	24,000	15.50	4.72	1.31
Image 3	June 20, 2019	4,790	10.27	3.13	< 1.00
Image 4	July 20, 2019	2,660	8.97	2.73	< 1.00

threshold values from Mahoney and Rood (1998), a disturbance event with RI values falling within the favorable category of cottonwood recruitment would need to range from 6.49 m (5-yr RI) to 7.16 m (10-yr RI). Whereas a marginal category or 3-yr RI begins at 6.05 m. Using the stage-height data from the USGS gage, the calculated recession rate indicates a recession rate over 36 days was approximately 7.6 cm/day which falls within the range of marginal values given in the literature (Table 5).

Geospatial Analysis

Calculation of RE_n facilitates the possibility of generating a spatially explicit map detailing cottonwood recruitment potential broken down by segment numbers. The estimated

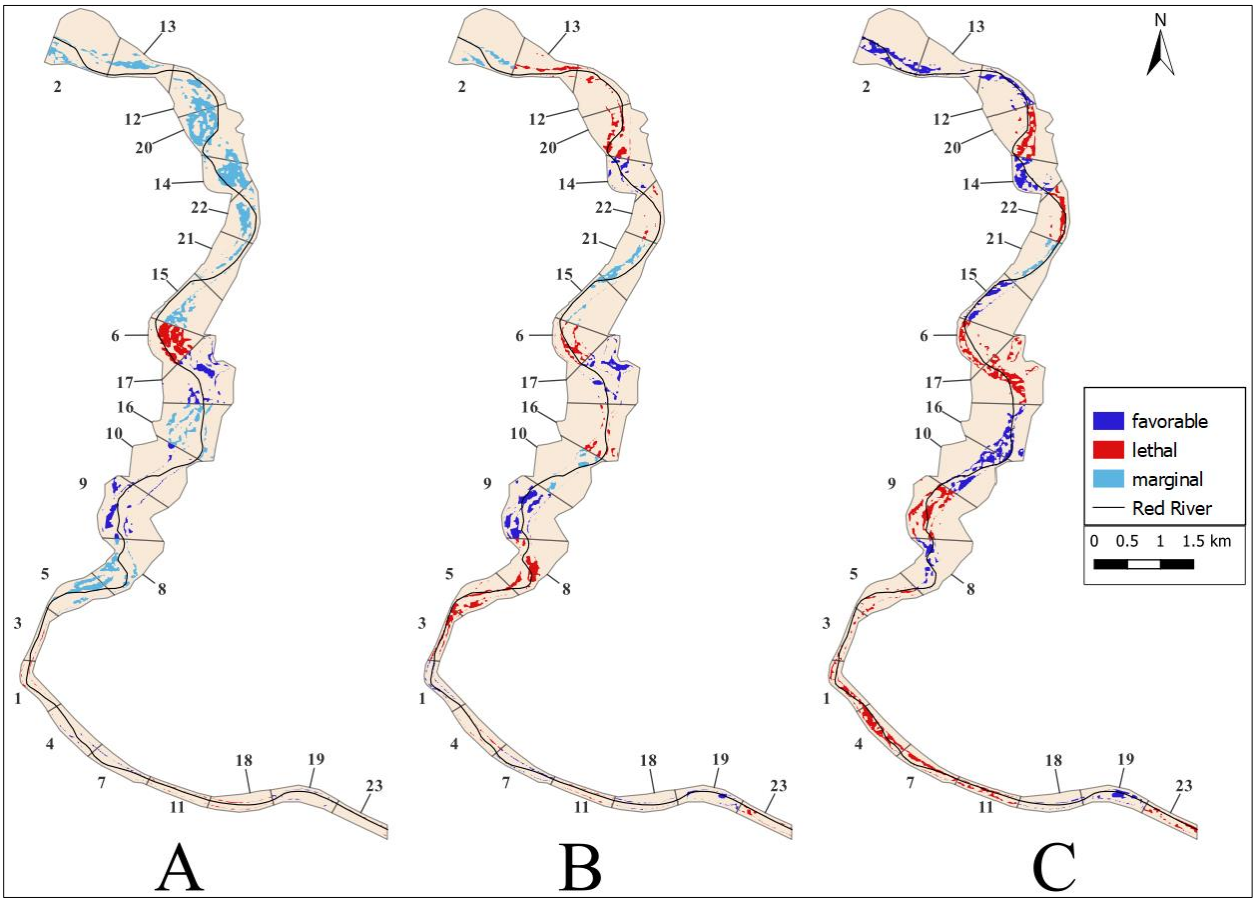

Figure 11. Geospatial Illustration of potential cottonwood recruitment areas, (A) recession extent #1 (RE_1), (B) recession extent #2 (RE_2), and (C) recession extent #3 (RE_3). Application: QGIS 3.22.3

favorability (Table 6) for each of the three calculated recession extents (RE_n) broken down by segment number can be spatially illustrated (Figure 11). The initial magnitude of floodplain intrusion can be shown by illustrating the difference in the WSE boundary between image 1 and image 2 (recession extent #1 or RE_1) (Figure 11.A). The areas color-coded as blue or light blue are areas that represent favorable and marginal cottonwood recruitment areas, respectively. All other areas are color-coded red and are categorized as unfavorable positions based on the results of the model. Recession extent #2 (RE_2) represents the difference between image 2 and image 3 (Figure 11.B). The interpretation of potential cottonwood recruitment areas within each extent follow the same color codes (Figure 11.A-C). Similarly, recession extent #3 (RE_3) is represented as the WSE boundary extent difference between image 3 and image 4 (Figure 11.C).

The overall recession extent and the favorability of cottonwood recruitment areas are based on the sequential evaluation of the all recession extents (Figure 12). Only one of the 23 segments shows a favorable cottonwood recruitment area based on the calculated recession metrics from the presented method which was segment #19. Segment #19 lies towards the end of the reach extent which includes the USGS gage location. The results of the presented method has identified only five segments of the 23 as marginal cottonwood recruitment areas while 17 segments were deemed unfavorable areas for recruitment. The geospatial analysis appears to support the marginal event status determined by the initial calculated recession rate of 7.6 cm/day over 36 days for the entire extent as most of the areas have been categorized as either lethal or marginal (Figure 12).

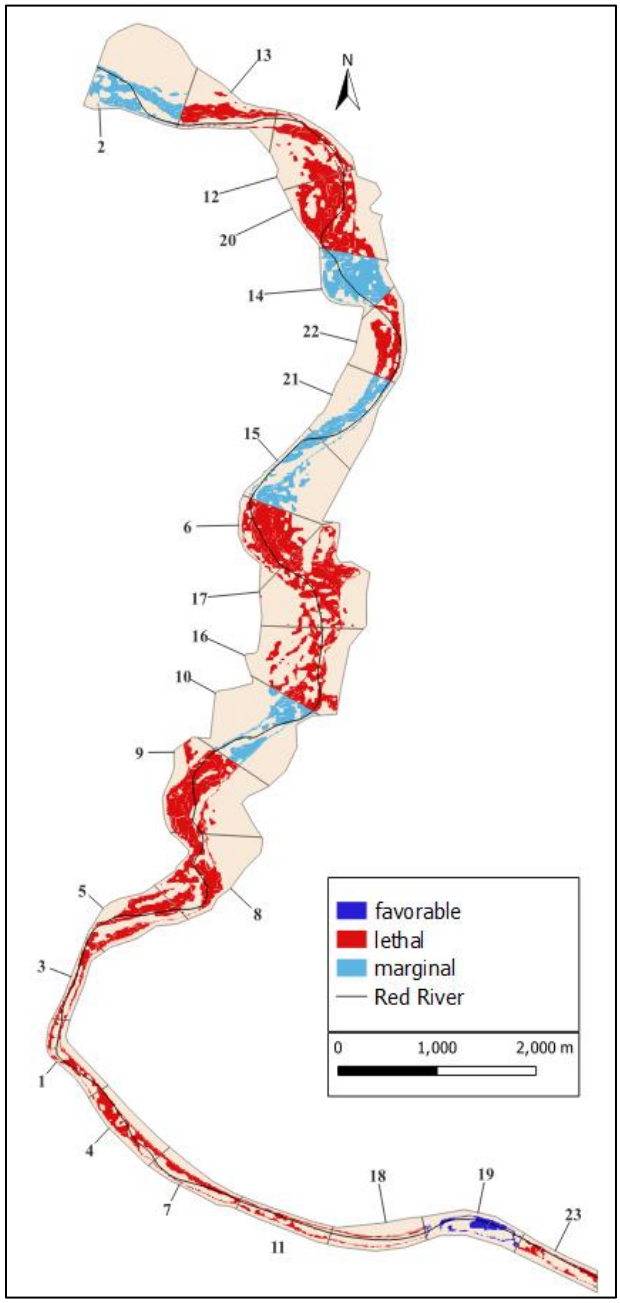

Figure 12. Geospatial illustration of potential areas of cottonwood recruitment based on the method thresholds with sequential evaluation of the recession extents (#1-3). Application: QGIS 3.22.3

DISCUSSION

Method Limitations

Successful cottonwood recruitment involves a complex array of ecohydrological processes that are intertwined spatially and temporally (Figure 1). It is inevitable the performance of the presented method will be limited by a variety of factors, including: correctly identifying the disturbance regime, uncertainty with remotely sensed data products, and encountering geospatial nuances within the analysis. In light of the many potential limitations that constrain my presented method's precision and performance, the method seems to have performed reasonably well.

Method Analysis

Given the method aligned with my performance expectations, recognizing the disturbance event could arguably be classified as an unfavorable cottonwood recruitment event and any conclusions drawn would be open for discussion is critical to improving the method performance. An area where the method needs refinement is its ability to take into account specific cottonwood recruitment scenarios that could potentially change a classification of a particular segment. My presented method indicated six of the 23 segments being classified as favorable or marginal for cottonwood recruitment potential (Table 6; Figure 12). The method presents a basic sequential analysis of recession rates without inputs from other variables that could steer a result one way or the other. For example, segment #13 and segment #16 (Figure 9), both present similar situations where the overall recession rate was classified as being a lethal area for cottonwood recruitment. Both segments were classified as having a marginal recession rate classification for RE_1 (7.5 and 5.8 cm/day, respectively), a lethal classification for RE_2 (0.0

cm/d for both), and a favorable classification for RE_3 (1.7 cm/d for both). The event did not indicate a change in recession from image 2 to image 3 thus producing a lethal classification for RE_2 with a recession rate of 0.0 cm/day result. Due to RE_2 being classified as lethal, the recruitment method selected a lethal overall result for the entire 36 day period. A lethal classification to a segment that did not have a recession to the WSE from the second recession extent (RE_2) is a bit premature. Both segments showed a noticeable change in the recession rates between image 1 and 2 with a marginal classification designation for RE_1. RE_1 represents a critical WSE as these areas are most likely to see cottonwood recruitment due to floodplain intrusion and possible scouring of vegetation. Thus, if the event has shown to recede at a level conducive for cottonwood recruitment per the established thresholds, then the lack of a recession in RE_2 should have little impact on seedling growth occurring within the RE_1 boundaries. In addition, a favorable recession in RE_3 supports continued growth and root elongation of cottonwood recruited within the boundaries of RE_1. In its current state, the recruitment method is limited in accurately determining the overall classification of a segment of interest. Weighting the extents with RE_1 having more significance than RE_2, and RE_3 could potentially reduce some of the classification errors in the current recruitment method iteration. Moving the recruitment method forward would need a more robust classification scheme to accurately predict cottonwood recruitment potential.

Validating a cottonwood recruitment classification scheme relying exclusively on geospatial analysis will be limited without the presence of ground truth data. By having ground-truthed data available, not only does the recruitment method receive a source of validation but can also contribute to calibrating the recruitment method to different types of riparian systems.

An ambitious end goal for this recruitment method is to produce a readily available map representing an accurate depiction of cottonwood recruitment areas supported by ground-truth data. Ground-truthed data is critical for a robust scientific model to produce results that are not only reliable but also increases the likelihood of repeatability.

Digital Elevation Model

By using remoted sensed data products, uncertainty within the data itself is a significant limiting factor to the performance of a given model. Using SAR data products in the manner I have presented, a digital elevation model (DEM) acquired during and/or immediately after the flow event would have been ideal to reduce some of the uncertainty associated with the calculated WSE elevation bands. Lotic dynamics dictate that river segments are not static features as sedimentation, sinuosity, and stream bank mobility frequently lead to changes in stream morphology. With a mobile stream channel, a single DEM used within the methodology can constrain model precision as the elevation band for a specific WSE is likely not correct for the flow event in question. Only one DEM product, acquired in 2018, was used which is well before the chosen high flow event. The DEM data points within the extent study area were likely different between the high flow event and the time of acquisition thus leading to significant uncertainty in the calculated elevation band for a segment of the WSE boundary. For example, segment #6 (Table 6) has a calculated recession rate of -5.0 cm/day. The negative number represents a significant increase in the WSE boundary elevation band between RE #1 and RE #2 suggesting that the water level rose. Intuitively, without any additional water inputs into the system, a rise in the water level 12 days after the peak is highly unlikely. This particular anomaly can best be explained as a channel migration event (or streambank collapse) where the

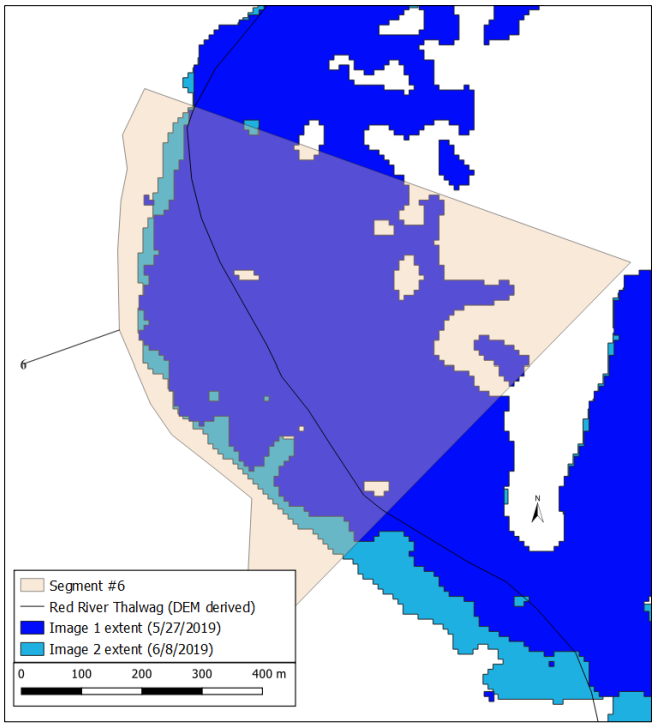

Figure 13. Channel migration event within the Segment #6 boundaries. Image 1 (dark blue) represents the peak of the high flow event, and image 2 (light blue) is the high water extent 12-days later.

movement of the WSE boundary had migrated into an area where the DEM was not up to date with the channel movement (Figure 13). Thus, when the calculation of the elevation band for segment #6 WSE boundary was performed, the data showed an increase in elevation from 245.4 m to 246.0 m. The model was able to quantify the elevation band correctly. However, due to the inaccurate elevation data points associated with the DEM and the WSE boundary, the model would need to be further refined to recognize migration events and reclassify such events as undetermined rather than being a lethal event.

Due to the uncertainty associated with the DEM product, precise calculation using the quantile method for selecting an elevation band will also be a source of contention. The quantile method is a simple and intuitive means of quickly establishing a single elevation value for an

entire WSE boundary. However, with areas of the DEM likely to be incorrect, establishing a precise elevation value can be problematic and limit the usefulness of the model results. The quantile method must be re-evaluated during the quality control process to establish a reasonable elevation value for each WSE elevation band as was done for some of the segments in this study.

Synthetic Aperture Radar C-Band

For over 40 years, there have been a number of satellites utilizing SAR sensors as the first L-Band SAR satellite was launched in 1978 with the SEASAT-1 mission (EOP, 2022). However, access to and the development of SAR processing techniques for Earth resource observation has been rather limited in the scientific community. Recently, the momentum of scientific inquiry regarding SAR-based inquiries has rapidly progressed in the refinement of techniques for improving the quality of SAR products due in large part to the open-access of Sentinel 1 datasets. A limitation to SAR data is related to the significant uncertainty inherent with the data itself as a SAR product can be quite noisy with signal strength irregularities, distortions of physical features, and processes related to the operational frequency. The operational frequency of SAR sensors are characterized by their different sensitivities (Figure 16, Appendix B) to surface features with each having a different utility and resolution (NASA, 2022) The C-band SAR signal has difficulty penetrating the vegetation canopy limiting its utility to higher order lotic systems. The inability of C-band SAR signal to penetrate the upper canopy of a riparian forest tends to mask water features that may be present below. The inability to acquire riparian understory data significantly reduces the utility for fine-scale ecohydrological analysis using a C-band SAR product.

Also, due to the loss of spatial resolution in the processing of SLC SAR products to the GRD SAR products, a 10-m spatial resolution represents a source of significant uncertainty for fine to moderate-scaled inquiries. Deriving an elevation band from a SAR derived WSE extent relies heavily on interpolating elevation data points along the length of the WSE extent. Using a DEM with a spatial resolution that does not match (i.e. 1 m or 30 m) the GRD SAR spatial resolution increases the amount of uncertainty related to deriving a WSE elevation band as some elevation data points are likely to be extrapolated thus leading to areas with erroneous data. To minimize the amount of possible error associated with the spatial resolution between the GRD SAR product and the DEM, I chose a 10-m DEM product as the best possible product to compare with the WSE boundaries.

Disturbance Event

A requirement for cottonwood recruitment is the need to identify and quantify a disturbance of sufficient magnitude resulting in scoured areas within a flood plain immediately preceding cottonwood or during seed dispersal. Mahoney and Rood (1998) suggested that a flow event of sufficient magnitude between a 5 to 10 year recurrence interval (RI) would likely produce favorable cottonwood recruitment areas, while Braatne et al. (2007) and Foster et al. (2018) suggest the range of flow-events is larger where the lower end of the RI could be as low as 3. RI values between 3 and 5 could be classified as a marginal event and result in limited areas for cottonwood recruitment. For the high flow event I chose to evaluate, the marginal category or 3-yr RI begins at 6.05 m which is higher than the peak of 5.46 m recorded by the USGS gage for the May 27, 2019 event (Table 7). The high-flow event presented in this study does not appear to meet a low-end marginal event threshold based on the RI values presented.

The RI metric seems to be a relatively weak disturbance indicator to predict cottonwood recruitment potential as the results of the study demonstrated the favorability of recruitment was present with an event that did not meet the RI threshold established from the literature. The focus of my study has been to present a framework workflow to predict cottonwood recruitment potential while utilizing an event that coincided with cottonwood seed dispersal and calculated recession from the available USGS gage data. Rather than using the RI as metric within the study, calculating a flow event's shear-stress appears to be a far superior metric indicator with regards to the impact of a disturbance (Benjankar et al., 2014; Benjankar et al., 2020). However, to incorporate a shear-stress metric into the model data would require knowledge of channel substrate and morphology which requires considerable amount of time and expense to gather the necessary field data. Recognizing the limited utility in the RI metric to set initial thresholds for whether or not a particular disturbance event is likely to result in cottonwood recruitment potential is nonetheless significant as RI can be helpful to guide an analyst to an appropriate event. In other words, the RI metric should be used to simply identify and quantify a particular flow event while understanding that such a metric may not be reliable in cases of cottonwood recruitment predictability.

Riparian Systems

The degradation of riparian areas due to human influence continues to be an environmental issue where solutions have seemingly failed to strike a balance between human interest and ecological integrity. Many restoration or mitigation activities tend to be localized or performed at the field-scale level with equivocal results as many landscape-scale variables are rarely assessed or evaluated as to their potential influence. Localized areas of riparian

mitigation/restoration must account for influencing variables at the landscape-scale for any restoration-type activity to be deemed successful. While not comprehensive, the methodology presented here is but a framework model needing further refinement to evaluate the ecological significance phreatic forest stands have on riparian integrity. In other words, cottonwood stands at the landscape-scale play a significant role within a localized riparian zone where conditions are conducive for recruitment, even without the presence of cottonwood. The presence of upstream cottonwood stands can influence landscape-scale processes where the upstream ecohydrology subsequently influences downstream geomorphology, flow rates, biotic assemblages and potential recruitment sites.

The methodology I present here is relatively straightforward and by no means exhaustive but highlights the evaluation of a critical metric (recession rate) necessary for cottonwood recruitment at the landscape scale. Interestingly, one segment out of 24 segments in the study produced a favorable recession rate for cottonwood recruitment in light of the low magnitude of disturbance. The disturbance was below the low-end marginal event established by the literature thresholds and likely would have not been given much attention for cottonwood recruitment potential based upon the established metrics. By isolating the critical metric (recession rate) for cottonwood recruitment potential using SAR data products, my method aligned favorably with my expectations in identifying landscape-scale recruitment areas. Ideally, having ground-truthed data available to validate the performance of my method will provide greater insight to the reliability of the method to predict areas of cottonwood recruitment. Currently, only a qualitative assessment of the method performance related to cottonwood recruitment can be presented. A more exhaustive analysis would include a multi-temporal evaluation of the

ecohydrological processes that constrain cottonwood recruitment and survival. Generally, a multi-year analyses will provide greater insight to the predictability of cottonwood recruitment as storm events during the fall months can prove to be lethal to cottonwood seedlings recruited months earlier.

CONCLUSION

Context & Future Considerations

The results of my study suggest the presented cottonwood recruitment methodology aligned very well with my expectations given the magnitude of the chosen event. Identification of water surface extents (WSE) using synthetic aperture radar (SAR) data is a well-established tool for flood mapping. By establishing an elevation band to the derived WSE, calculating a recession rate that aligned with established threshold metrics for cottonwood recruitment was a relatively straightforward process. Thus, I was able to successfully produce a spatiotemporal illustration of areas of potential cottonwood recruitment using SAR-based WSEs. However, my presented methodology is not a finished product and will need further refinement in identifying potential recruitment areas with greater accuracy and precision. Two immediate goals that will merit consideration in future recruitment method iterations include mitigating factors related to uncertainty in the data, and exploring the use of L-band SAR products to improve the performance of the method. First, an evaluation of cottonwood recruitment should not focus just on data surrounding a single event. Rather, an evaluation of multiple high flow events occurring across all seasons over a 2-year time frame from the initial recruitment event would yield greater precision and accuracy in the prediction of cottonwood recruitment areas (Foster et al., 2018). Second, due to the limited canopy penetration offered by C-band SAR sensitivities, much of the riparian area in the focal area of this study is comprised of forested areas likely resulting in some discontinuities with the WSE boundaries (Figure 4). L-band SAR products operate on a longer wavelength than the C-band data product (Figure 16 – Appendix B) and are likely to evaluate forested riparian areas more effectively by penetrating the upper canopy and deriving more

precise WSEs (Saatchi, 2019). By using an L-band SAR product, ecohydrological inquiries of systems with lower order tributaries where the WSEs are covered by riparian vegetation seem more plausible to explore further.

My study is by no means comprehensive, but is a step in the right direction to contribute to a greater understanding of ecohydrological processes at the landscape-scale. There seems to be a growing number of studies devoted to the SAR-based or LiDAR-based ecological inquiries at a broad scale regarding cottonwood recruitment such as those presented by Benjankar et al. (2018a and 2018b). For most cottonwood recruitment studies, the scale of most inquiries are limited to transect evaluations in the field and reliance on upscaling these fine-scale results to a broad area. Mahoney and Rood (1998), Braatne et al., (2007), and Foster et al. (2018) present excellent articles regarding fine-scale analysis of cottonwood recruitment and are quite useful but have a limited utility for broad-scale applications. The problem is that these studies become limited in their application due to the heterogeneity of the landscape at broad scales thus necessitating a need for broad-scale applications such as the method I have presented here. The method I have presented can help improve understanding of cottonwood phenology as well as enhance the broader understanding of riparian vegetation dynamics in an anthropogenic system.

REFERENCES CITED

Atchafalaya National Heritage Area (ANHA), 2022. Water Heritage: Atchafalaya Basin at http://www.atchafalaya.org/atchafalaya-basin. Accessed on January 25, 2022.

Baldys, S. & Phillips, D. (1997). Stream monitoring and educational program in the Red River basin, Texas, 1996-1997. United States Geological Society, Fact Sheet, 170-97. Access on January 25, 2022 at https://pubs.usgs.gov/fs/fs-170-97/.

Benjankar, R., Burke, M., Yager, E., Tonina, D., Egger, G., Rood, S., & Merz, N. 2014. Development of a spatially-distributed hydroecological model to simulate cottonwood seedling recruitment along rivers. *Journal of Environmental Management, 145*, 277-288.

Benjankar, R., Tranmer, A., Vidergar, D., & Tonina, D. 2020. Riparian vegetation model to predict seedling recruitment and restoration alternatives. *Journal of Environmental Management, 276*, 111339.

Bertoldi, W., Drake, N., & Gurnell, A. 2011. Interactions between river flows and colonizing vegetation on a braided river: Exploring spatial and temporal dynamics in riparian vegetation cover using satellite data. *Earth Surface Processes and Landforms, 36*(11), 1474-1486.

Bouaraba, A., Belhadj-Aissa, A. & Closson, D., 2018. DRASTIC IMPROVEMENT OF CHANGE DETECTION RESULTS WITH MULTILOOK COMPLEX SAR IMAGES APPROACH. Progress in electromagnetics research C Pier C, 82, pp.55–66.

Braatne J., Rood S., & Heilman P. 1996. Life history, ecology, and reproduction of riparian cottonwoods in North America. In: Stettler RF, Bradshaw Jr HD, Heilman PE, Hinckley TM (eds). Biology of Populus and its Implications for Management and Conservation. NRC Research Press: Ottawa, Canada. pp 5785.

Braatne, J., Jamieson, R., Gill, K., & Rood, S. 2007. Instream flows and the decline of riparian cottonwoods along the Yakima River, Washington, USA. *River Research and Applications, 23*(6), 247-267.

Brown, J. & Hogan, D. 2020. SAR-101: An introduction to synthetic aperture radar. Capella Space at https://www.capellaspace.com/sar-101-an-introduction-to-synthetic-aperture-radar/. Accessed Septmeber 6, 2021.

Burke, M., Jorde, K., & Buffington, J. 2009. Application of a hierarchical framework for assessing environmental impacts of dam operation: Changes in streamflow, bed mobility and recruitment of riparian trees in a western North American river. *Journal of Environmental Management, 90*, S224-S236.

Cian, F., Marconcini, M. & Ceccato, P., 2018(a). Normalized Difference Flood Index for rapid flood mapping: Taking advantage of EO big data. Remote sensing of environment, 209, pp.712–730.

Cian, F., Marconcini, M., Ceccato, P., & Giupponi, C. 2018(b). Flood depth estimation by means of high-resolution SAR images and lidar data. Natural hazards and earth system sciences, 18(11), pp.3063–3084.

Elizavetin, I. (2010). Radiometric artifacts on SAR images (presentation). International Technical and Scientific Conference. Gaeta, Italy. September 2010.

Earth Observation Portal (EOP). 2022. Seasat mission: the world's first satellite mission dedicated to oceanography. European Space Agency at: https://directory.eoportal.org/web/eoportal/satellite-missions/s/seasat. Accessed on March 14, 2022.

European Space Agency (ESA). 2022. Sentinel 1 SAR User Guide at https://sentinels.copernicus.eu/web/sentinel/user-guides/sentinel-1-sar. Accessed on August 9, 2021.

Filipponi, F. 2019. Sentinel 1 GRD Pre-processing workflow. International Electronic Conference on Remote Sensing. Roma, Italy. June 4, 2019.

Foster, S., Mahoney, J., & Rood, S. 2018. Functional flows: An environmental flow regime benefits riparian cottonwoods along the Waterton River, Alberta. *Restoration Ecology*, 26(5), 921-932.

Lee, J.S., Jurkevich, L, Dewaele , P., Wambacq, P., & Oosterlinck, A. (1994) Speckle filtering of synthetic aperture radar images: A review, Remote Sensing Reviews, 8:4, 313-340,

Lillesand, T.M.; Kiefer, R.W.; Chipman, J.W. Remote Sensing and Image Interpretation, 7th ed.; John Wiley &Sons, Inc.: Hoboken, NJ, USA, 2015.

Long, S., Fatoyinbo, T.E. & Policelli, F., 2014. Flood extent mapping for Namibia using change detection and thresholding with SAR. Environmental research letters, 9(3), p.35002.

Mahoney, J., & Rood, S. 1998. Streamflow requirements for cottonwood seedling recruitment—an integrative model. *Wetlands (Wilmington, N.C.), 18*(4), 634-645.

National Aeronautics and Space Administration (NASA). 2022. What is SAR? Earthdata for open access for open science accessed at: https://earthdata.nasa.gov/learn/backgrounders/what-is-sar. Accessed January 25, 2022.

O'Neill, R.V., DeAngelis, D.L., Waide, J.B., & Allen, T.F.H. 1986. A Hierarchical Concept of Ecosystems. Princeton University Press, Princeton.

Poff, N., Allan, J., Bain, M., Karr, J., Prestegaard, K., Richter, B., Sparks, R., & Stromberg, J. 1997. The natural flow regime: A paradigm for river conservation and restoration. *Bioscience, 47*(11), 769.

RStudio Team (2022). RStudio: Integrated Development for R. RStudio, PBC, Boston, MA URL http://www.rstudio.com/.

Rood, S., Braatne, J., & Hughes, F. 2003. Ecophysiology of riparian cottonwoods: Stream flow dependency, water relations and restoration. *Tree Physiology, 23*(16), 1113-1124.

Rood, S., & Kaluthota, S. 2020. Cottonwood Seed Dispersal Phenology across North America and Worldwide: Tracking 'Summer Snow' through an Internet Search. *Wetlands* (Wilmington, N.C.), 40(6), 1935-1947.

Saatchi, S. 2019. SAR Methods for Mapping and Monitoring Forest Biomass. SAR Handbook: Comprehensive Methodologies for Forest Monitoring and Biomass Estimation. Eds. Flores, A., Herndon, K., Thapa, R., Cherrington, E. NASA.

Sipelgas, L., Aavaste, A. & Uiboupin, R., 2021. Mapping Flood Extent and Frequency from Sentinel-1 Imagery during the Extremely Warm Winter of 2020 in Boreal Floodplains and Forests. Remote sensing (Basel, Switzerland), 13(23), p.4949.

Texas Almanac, 2022. Major Rivers at https://www.texasalmanac.com/articles/rivers. Accessed January 25, 2022.

U.S. Geological Survey (USGS), 2022. National Water Information System: Web Interface at https://waterdata.usgs.gov/nwis/inventory?site_no=07316000 accessed January 18, 2022.

Zamani Sabzi, H., Moreno, H., Fovargue, R., Xue, X., Hong, Y., & Neeson, T. 2019. Comparison of projected water availability and demand reveals future hotspots of water stress in the Red River basin, USA. Journal of Hydrology. Regional Studies, 26, 100638.

APPENDIX A

GROUND RANGE DETECTED SYNTHETIC APERTURE RADAR: GEOMETRY AND DISTORTIONS

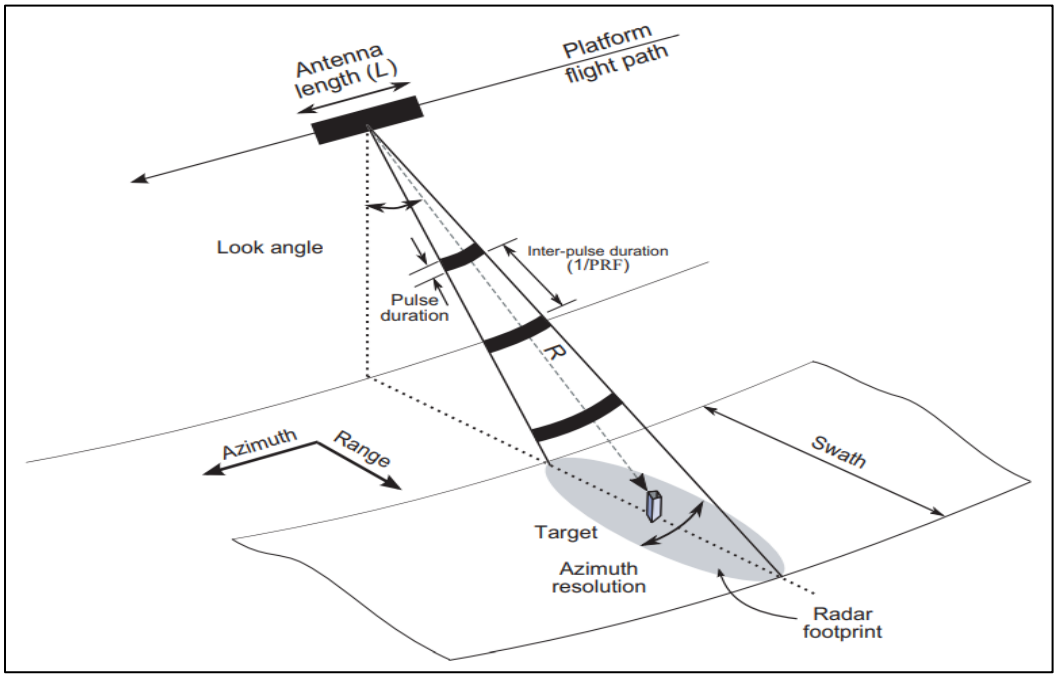

Figure 14. Synthetic Aperture Radar Geometry. Source: Bouaraba et al. 2018

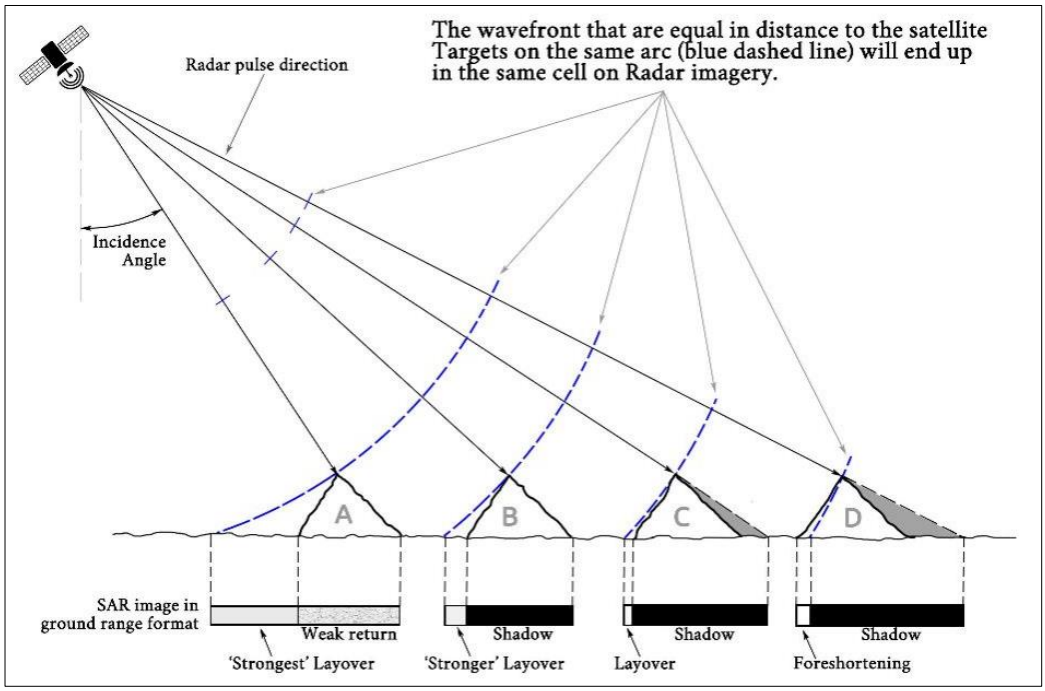

Figure 15. Geometric distortion effect (foreshortening, layover, and shadowing) from terrain features using SAR imagery. Souce: Lillesan et al. 2015..

APPENDIX B

SYNTHETIC APERTURE RADAR (SAR) SENSITIVITY BANDS

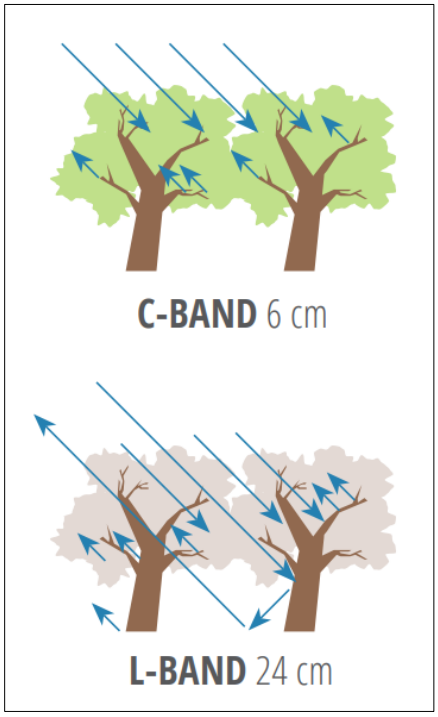

Figure 16. SAR sensitivity, canopy penetration comparison between C-band and L-Band wavelengths. Source: Saatchi, 2019